Numerical Investigation on Amphibious UAV Using Turbulent Models for Drag Reduction

P. Gokul Raj , Balasubramanian Esakki, P. Vikram, and Lung-Jieh Yang

Abstract Unmanned Aerial Vehicles (UAVs) have gained significant consideration lately because of its flexibility in arrangement for multiple activities. Especially amphibious UAVs' integration of air cushion vehicle and multirotor has huge demand in military, maritime and seaside protection applications. Steadiness and execution of these sorts of vehicles profoundly rely upon streamlined cooperation of multirotor regarding different wind conditions. The present work focuses on limiting the drag and enhancing the streamlined execution attributes. CFD examination is performed through considering different turbulent models such as k-ω, k-ε and SST k-ω (shear pressure transport) to assess the co-efficient of drag of amphibious UAV. Static investigation is performed through varying the Angle of Attack (AoA) from 0° to 10° under relative velocities of 3, 5, 8 and 10 m/s. The turbulence kinetic energy shapes anticipated the streamline of wind stream around the vehicle.

Keywords Amphibious UAV · CFD · RANS model · Drag · Blunt body

P. Gokul Raj · B. Esakki (✉)
Department of Mechanical Engineering, Vel Tech Rangarajan Dr. Sagunthala R&D Institute of Science and Technology, Avadi, Chennai 600062, India
e-mail: esak.bala@gmail.com

P. Gokul Raj
e-mail: gokulrajprithiv@gmail.com

P. Vikram
Department of Aeronautical Engineering, Vel Tech Rangarajan Dr. Sagunthala R&D Institute of Science and Technology, Avadi, Chennai 600062, India
e-mail: Vikram.veeran@gmail.com

L.-J. Yang
School of Mechanical and Electro Mechanical Engineering, Tamkang University, New Taipei City, Taiwan
e-mail: ljyang@mail.tku.edu.tw

1   Introduction

Unmanned Aerial Vehicles (UAVs) are dominatingly utilized in various applications [1, 2] including accuracy agribusiness, environmental monitoring, aerial imaging, pursuit and protection, observation and surveillance, control line and telecom tower assessments and so on. Be that as it may, the use of UAVs in water quality checking and gathering of water tests in remote water bodies is rare. A UAV which can fly, land and skim along the water surface forcing parcel of difficulties as far as control in flight transition, selection of materials, propulsion, energy consumption and pay load capacity [3]. Also, different factors, for example, as durability, reliability, safety and minimal cost, are utmost important for industrial demand and client necessity. There are few drifting UAVs which have been produced and popularized in the market [4]. These vehicles are planned to cover substantial regions of water bodies in limited ability to focus time. In contrast to other gliding vehicles, because of the guideline of air cushion vehicle [5], the erosion between the vehicle and water surface is kept away, thereby gigantic measure of vitality is spared. The vertical take-off and landing capacity of vehicle can position the vehicle in exact water areas crosswise over waterways, lakes and other water bodies to perform water quality analysis. One of the streamlined parameters affecting continuance of land and/or water capable vehicle is drag. There are few investigations led to ascertain the drag of fixed wing and rotating wing vehicle. Sitaraman and Baeder [6] completed streamlined investigation of quadrotor utilizing Navier–Stokes condition, and wake associations are considered. Steijl et al. [7] contemplated rotor and fuselage collaboration utilizing CFD investigation and sliding plane procedure [8]. The fierce stream qualities amid inviscid and viscid liquids are re-enacted in CFD to dissect the conduct of covers of multirotor framework. Biava et al. [9] inspected the streamlined conduct of helicopter through CFD and exploratory examinations. Kusyumov et al. [10] completed CFD examination of ANSAT helicopter to decide lift and drag powers in viscous flow conditions. Yoon et al. [11] dissected stream appropriation over settled wing aerofoil through shifted AoA and co-effective of drag and lift is obtained. Abudarag et al. [12–15] considered the stream partition among rotor and fuselage utilizing CFD, and fierce stream attributes are analysed. The present work focuses on performing CFD analysis of various tempestuous models, for example, k-ω, k-ε and SST k-ω to determine the co-efficient of drag under different AoA and relative velocity conditions.

2   Modelling

The conceptualization amphibian model is designed through inculcating the principles of multirotor and hover craft as shown in Fig. 1. In order to reduce the computational effort, the model is scaled down to factor of 1:0.25. Also, to maintain the
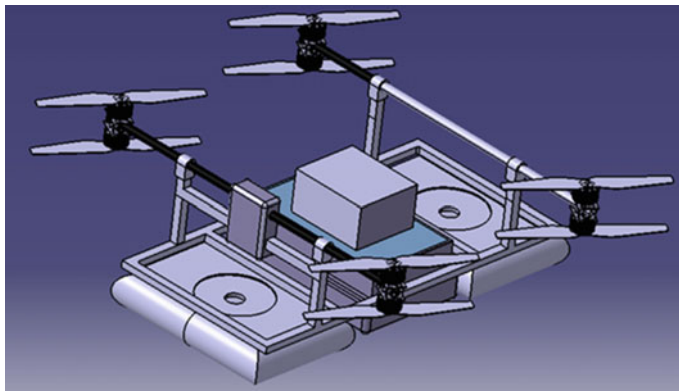
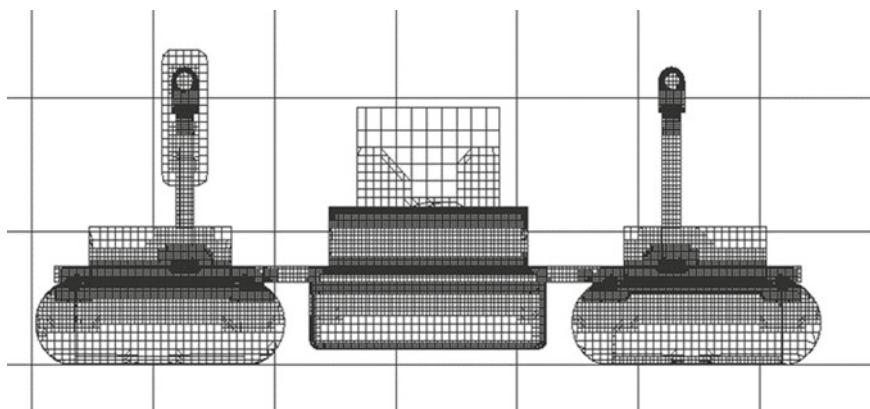**Fig. 1** Conceptualized model of amphibious vehicle

Fig. 2 Structured mesh of the scaled-down amphibious vehicle

Reynolds number with reference to the prototype, velocity is increased four times and various wind speed conditions are accounted for simulation studies.

The scaled-down amphibian structure is meshed with cut-cell element using ICEM tool. Grid quality is verified with skewness and orthogonality checks. The structured meshed image of the scaled-down model is as shown in Fig. 2.

3　Computational Fluid Dynamic Analysis

CFD analysis is performed through varying the AoA (0°–10°) under various relative air velocity conditions. Simulation studies are conducted for the following four cases of velocity conditions.
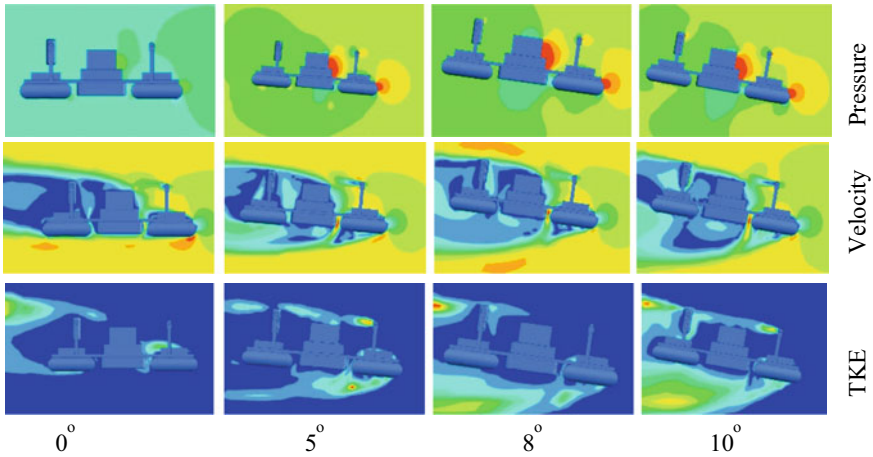
Case 1: 3m/s

Fig. 3 Velocity, pressure and turbulence kinetic energy contours at 3 m/s for different AoA

Case 1: 3 m/s

At 0° AoA, high turn around stream district is happened behind the water sampler module. While expanding the AoA, the velocity is streamlined and at 8° AoA, reverse flow around amphibious vehicle is streamlined which lessens drag (Fig. 3). Further, increment of AoA prompts arrangement of fierce area at the back of vehicle that may cause increment of the drag. It is clear from pressure contour of differed AoA is that up to 8°, there is a decline in pattern of weight, further increment of AoA causes increment in pressure in the upstream district, and there is a probability of instability of vehicle. Additionally, over 8° of AoA, kinematic energy disturbance is expanded which may prompt vibration and unfit to control the vehicle in the ideal way.

Case 2: 5 m/s

Similar phenomenon is observed as in the case of 3 m/s. However, the intensity of velocity and pressure is quite high as compared to 3 m/s (Fig. 4).

Case 3: 8 m/s

Figure 5 shows the variation velocity, pressure and turbulence kinematic energy contours at 8 m/s for all the four different AoA.

Case 4: 10 m/s

The intensity of turbulence is increased at high relative air speed which can be seen in Fig. 6. For various wind speed conditions and AoA, the co-efficient of drag and lift is estimated which is given in Table 1. It is observed that increase in AoA and wind speed causes increase in drag and decrease in lift. The lift-to-drag ratio for the wind speed of 8 m/s given in Table 2 reveals that at 5° AoA, high amount of lift is generated with minimal drag.

For various turbulent models such as k-ω, k-ε and SST k-ω, CFD analysis is performed and corresponding drag force is determined. Since k-ω is considered as a
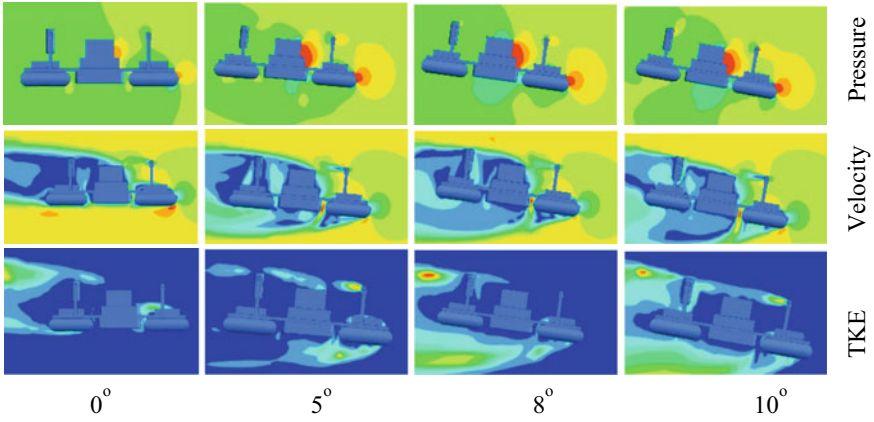
Case 2: 5m/s

Fig. 4 Velocity, pressure and turbulence kinetic energy contours at 5 m/s for different AoA
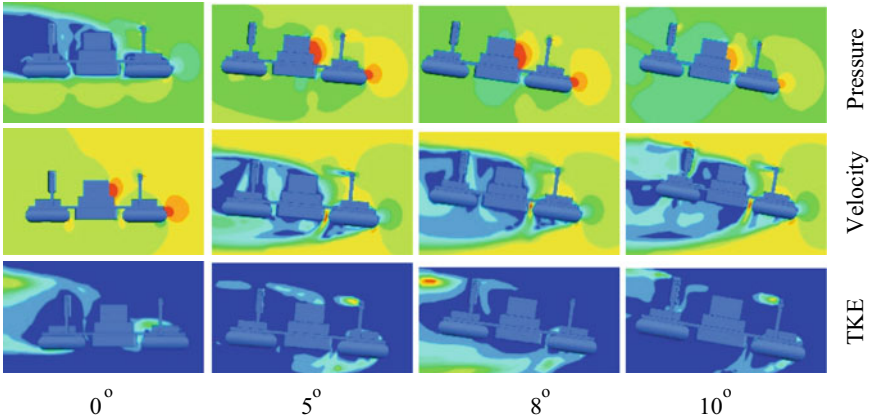
Case 3: 8m/s

Fig. 5 Velocity, pressure and turbulence kinetic energy contours at 8 m/s for different AoA

standard model to measure the drag force, with reference to that error is calculated. Minimum error is obtained for these models which are given in Table 3, and they can be used to calculate the drag force.

4   Conclusion

CFD analysis is performed for the designed amphibian structure through varying the AoA from 0° to 10° under different wind speed conditions (3, 5, 8 and 10 m/s), and
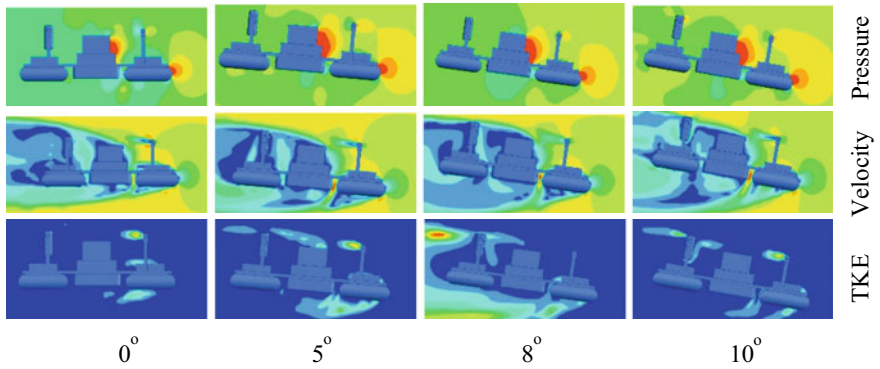
Fig. 6 Velocity, pressure and turbulence kinetic energy contours at 10 m/s for different AoA

Table 1 Estimation of drag for various AoA under different wind speed conditions

Wind speed (m/s)	Parameters	Angle of Attack			
		0°	5°	8°	10°
3	C_D	0.566	0.534	0.489	0.483
	C_L	0.164	0.171	0.083	0.082
	Drag	0.783	0.931	1.009	1.050
5	C_D	0.562	0.532	0.489	0.481
	C_L	0.159	0.172	0.086	0.075
	Drag	2.160	2.577	2.805	2.903
8	C_D	0.573	0.531	0.485	0.463
	C_L	0.152	0.173	0.081	0.023
	Drag	5.631	6.588	7.114	7.159
10	C_D	0.618	0.531	0.486	0.465
	C_L	0.123	0.172	0.081	0.080
	Drag	9.481	10.274	11.133	11.237

Table 2 Lift-to-drag ratio at 8 m/s

AoA (°)	Drag (N)	Lift (N)	L/D ratio
0	5.631	1.499	0.266
5	6.588	2.151	0.326
8	7.114	1.187	0.166
10	7.159	0.369	0.051

Table 3 Computation of drag using various turbulent models

AoA (°)	Relative velocity (m/s)	Drag (N) (k-ω model)	Drag (N) (k-ε model)	Drag (N) (SST k-ω model)	Error (k-ω/SST k-ω)	Error (k-ω/k-ε)
5	5	2.568	2.610	2.577	−0.009	−0.042
	8	6.572	6.619	6.588	−0.016	−0.047
8	5	2.770	2.784	2.805	−0.035	−0.014
	8	7.107	7.121	7.114	−0.007	−0.014

corresponding co-efficient of drag and lift force are calculated. At 8 m/s and 5° AoA, maximum L/D ratio is obtained in comparison to other operating conditions, and hence, it is well suited for cruise flight. Comparative evaluation of various turbulent models such as k-ω, k-ε and SST k-ω suggested that error between standard k-ω and other models is minimum, and hence, they can be also used for dynamic analysis.

References

1. Valavanis KP, Vachtsevanos GJ (2014) Handbook of unmanned aerial vehicles. Springer
2. Hassanalian M, Abdelkefi A (2017) Classifications, applications, and design challenges of drones: a review. Prog Aerosp Sci 91:99–131
3. Pisanich G, Morris S (2002) Fielding an amphibious UAV—development, results, and lessons learned. In: Digital avionics systems conference, vol 2, pp 8C4–8C4
4. Boxerbaum AS, Werk P, Quinn RD, Vaidyanathan R (2005) Design of an autonomous amphibious robot for surf zone operation: part I mechanical design for multi-mode mobility. In: Advanced intelligent mechatronics proceedings, IEEE/ASME international conference, pp 1459–1464
5. Amyot JR (2013) Hovercraft technology, economics and applications, vol 11. North Holland
6. Sitaraman J, Baeder J (2002). Analysis of quad-tiltrotor blade aerodynamic loads using coupled CFD/free wake analysis. In: 20th AIAA applied aerodynamics conference, p 2813
7. Steijl R, Barakos G, Badcock K (2007) CFD Analysis of rotor-fuselage aerodynamics based on a sliding mesh algorithm
8. Grondin G, Thipyopas C, Moschetta JM (2010) Aerodynamic Analysis of a multi-mission short shrouded coaxial UAV: part III-CFD for hovering flight. In: 28th AIAA applied aerodynamics conference, p 5073
9. Biava M, Khier W, Vigevano L (2012) CFD prediction of air flow past a full helicopter configuration. Aerosp Sci Technol 19(1):3–18
10. Kusyumov A, Mikhailov SA, Garipov AO, Nikolaev EI, Barakos G (2015) CFD simulation of fuselage aerodynamics of the ANSAT helicopter prototype. Trans Control Mech Syst 1(7):318–324
11. Yoon S, Lee HC, Pulliam TH (2016) Computational analysis of multi-rotor flows. In: 54th AIAA aerospace sciences meeting, p 0812
12. Abudarag S, Yagoub R, Elfatih H, Filipovic Z (2017) Computational analysis of unmanned aerial vehicle (UAV). In: AIP conference proceedings, vol 1798, no 1. AIP Publishing, p 020001
13. Lesieur M (1987) Turbulence in fluids: stochastic and numerical modelling. Nijhoff, Boston, MA

14. Versteeg HK, Malalasekera W (2007) An introduction to computational fluid dynamics: the finite volume method. Pearson Education
15. Ferziger JH, Peric M (2012) Computational methods for fluid dynamics. Springer Science & Business Media